

1988

An Analytical Model of Heat Transfer to the Suction Gas in a Low-Side Hermetic Refrigeration Compressor

William A. Meyer
Purdue University

H. Doyle Thompson
Purdue University

Follow this and additional works at: <https://docs.lib.purdue.edu/icec>

Meyer, William A. and Thompson, H. Doyle, "An Analytical Model of Heat Transfer to the Suction Gas in a Low-Side Hermetic Refrigeration Compressor" (1988). *International Compressor Engineering Conference*. Paper 662.
<https://docs.lib.purdue.edu/icec/662>

This document has been made available through Purdue e-Pubs, a service of the Purdue University Libraries. Please contact epubs@purdue.edu for additional information.

Complete proceedings may be acquired in print and on CD-ROM directly from the Ray W. Herrick Laboratories at <https://engineering.purdue.edu/Herrick/Events/orderlit.html>

AN ANALYTICAL MODEL OF HEAT TRANSFER
TO THE SUCTION GAS IN A LOW-SIDE HERMETIC
REFRIGERATION COMPRESSOR

William A. Meyer
Former Graduate Research Assistant
Presently at Synthes Maxillofacial
Paili, PA 19301
(215) 647-9700

H. Doyle Thompson
Dept. of Mechanical Engineering
Purdue University
W. Lafayette, IN 47907
(317) 494-5624

ABSTRACT

Heat transfer to the suction gas in a hermetic compressor is known to have adverse effects on compressor performance. This can be explained in an overall sense by thermodynamic cycle analysis. The extent of suction gas heated inside the compressor and the areas in which this heating occurs requires a more detailed heat transfer analysis.

The analytical model for this study is a small (about 1/3 horsepower), low-side, reciprocating, hermetic compressor. The heat transfer equations for this model are derived from steady-state energy balances on the overall system and on various compressor components. Where applicable, heat transfer coefficients are determined from correlations found in the literature. A volumetric efficiency and a compression efficiency are determined from the experimental data. Some of the heat transfer coefficients for the complex three-dimensional geometries were also determined from experimental measurements.

The model is used to predict the compressor performance over a range of operating conditions. Comparison with experimental measurements shows that the major trends are predicted by the model. Model adequacy and potential improvements are discussed.

INTRODUCTION

This paper deals with the operating efficiency of small, hermetically sealed, low side refrigeration compressors. More particularly, it concerns the heat transfer to the refrigerant gas in the flow passages between the suction line leaving the evaporator and the high pressure line leaving the compressor shell.

Any heat transfer to the refrigerant gas between the outlet of the evaporator and the intake to the compressor cylinder can be considered as wasted cooling capacity which reduces cycle efficiency. Theoretically, a simple, well insulated, direct connection between the suction line and the intake manifold would be the most efficient design. However, other considerations make the direct connection undesirable. Those considerations include noise propagation, the need to separate the compressor oil from the refrigerant gas, and slugging problems associated with start-up. In addition, the suction gas is used to cool the electric motor and compressor in some designs.

Figure 1 is a schematic showing the major internal components of a small, low side compressor which is the model for this study. Refrigerant gas enters the compressor shell through the suction line. During the intake stroke of the compression piston a fresh charge of refrigerant gas is drawn into the muffler, through the muffler, through the suction plenum, and into the compression cylinder. That gas is a mixture of unheated gas directly from the suction line and heated gas that has been circulating inside the compressor shell. During the compression stroke the suction gas entering the compressor shell spills around the muffler. This design has the desirable characteristic of damping the compressor noise. It also provides an easy method of separating oil drops from the refrigerant gas, and eliminates slugging problems. Theoretical estimates show that for the small compressor considered here, a 10F increase in suction gas temperature results in approximately a one percent decrease in compressor efficiency.

This paper is the result of a theoretical investigation that was undertaken to study the heat transfer to the suction gas at various stages inside the compressor shell. The details of the study are contained in Refs. 1 and 2. A parallel experimental study was also conducted to measure the temperatures, pressures, mass flow rate and power consumption for this compressor. In that study the effect of varying the temperature of the suction gas was investigated as was the effect of the compressor design. In the experimental study five different configurations were tested. They are a) the suction inlet and muffler inlet aligned (normal configuration), b) the muffler inlet offset by 1/4 inch from the suction inlet (offset configuration), c) the suction inlet on the opposite side of the compressor shell from the muffler (opposite configuration), d) the normal configuration with a shroud around the muffler to restrict the flow circulation (shroud-aligned configuration), and e) the offset alignment with a shroud (shroud-offset configuration). The details of the experimental study are contained in Refs. 1, 2, and 3.

A companion study used flow visualization to investigate the flow pattern of the suction gas in transit between the suction inlet and the muffler inlet. The flow pattern was recorded on video tape and compared for the following cases:

1. The muffler inlet in alignment with the suction inlet,
2. The muffler inlet misaligned relative to the suction inlet,
3. Different offset between the aligned muffler inlet and suction inlet,
4. The use of a shroud around the muffler to partially baffle the flow in the vicinity of the muffler, and
5. The use of a larger volume muffler instead of the standard muffler, with an increased inlet hole diameter and increased outlet passage diameter.

Reference 4 describes the flow-visualization study in detail, and also contains the video tape produced as part of that study. The work is also described in Refs. 5 and 6.

In this study an analytical heat transfer model of the compressor is developed. The effects of different suction line temperatures and the effects of compressor design changes are computed and compared to the measured results of Refs. 1, 2, and 3. The heat transfer model is developed by combining the energy and mass flow equations for a series of control volumes. The energy balances are for steady state operation. They include free and forced convection and radiation. Heat transfer coefficients for energy transfer from the compressor shell are determined from correlations in the heat transfer literature. Heat transfer coefficients for the gas inside the compressor shell are determined from experimental measurements. The correlations are described in detail in Refs. 1 and 2, and are discussed briefly in the next section.

ENERGY BALANCES

Energy balances are developed for

1. The overall compressor,
2. The refrigerant gas inside the compressor shell,
3. The muffler,
4. The discharge line,
5. The electric motor, the bottom of the compressor shell, and the lubricating oil, and
6. The top and sides of the compressor shell.

Overall Energy Balance

Figure 2 illustrates the control volume for the overall energy balance. The steady state energy equation, written as a rate equation is:

$$\dot{W} = \dot{Q} + \dot{m}(i_d - i_s) \quad (1)$$

where \dot{W} is the power input, \dot{Q} is the heat transfer rate from the compressor shell, \dot{m} is the mass flow rate, and i_d and i_s are the specific enthalpy of the discharge and suction gas respectively. In this analysis the power input is a known quantity, the specific enthalpy of the suction gas is determined from the specified temperature and pressure of the suction gas, and the specific enthalpy of the discharge gas is a function of the specified discharge pressure and the unknown discharge temperature. The mass flow rate is unknown at this point. To determine the heat transfer rate from the compressor shell, the shell is divided into three sections namely the top, sides, and bottom. The heat transfer modes are illustrated in Fig. 3. Forced convection was included for heat transfer from the top and sides of the shell so that the analysis would be consistent with the experimental results which used a cooling fan. Free convection and radiation to the ambient surroundings were included for all surfaces.

The eight heat transfer rates, \dot{Q}_i , illustrated in Fig. 3 can be put into the form,

$$\dot{Q}_i = h_i A_i (T_i - T_a) \quad (2)$$

where h_i is the appropriate heat transfer coefficient, A_i is the surface area, T_i is the effective surface temperature, and T_a is the ambient temperature. The areas, A_i , are known as is the ambient temperature, T_a . The surface temperatures are unknown. In this analysis the problem is simplified by assuming that the top and sides of the compressor shell are at the same temperature, T_{sh} , and that the bottom of the shell, the motor, and the compressor oil are at the same temperature, T_{mot} .

The forced and free convection heat transfer coefficients are determined from Nusselt number correlations with the Rayleigh, Reynolds and Prandtl numbers as described in Ref. 7.

For example the free convection heat transfer coefficients, h , for the top and bottom of the shell are determined using the correlation for a horizontal plate (see Ref.7, pg 445).

$$Nu = \frac{h D}{k_a} = C (Ra)^n \quad (3)$$

where D is the shell diameter, k_a is the thermal conductivity of the air, R_a is the Rayleigh number, and the constants C and n are determined as given in Ref. 7.

The correlation on page 442 of Ref. 7 was used to determine the free convection coefficient for the sides. The forced convection coefficients for the top and sides were determined from the correlations on Pages 344 and 330 respectively.

The radiation coefficients are of the form

$$h_{rad} = \epsilon \sigma (T_i + T_s) (T_i^2 + T_s^2) \quad (4)$$

where ϵ is the emissivity (assumed value of 0.9) and σ is the Steffan-Boltzman constant.

The unknowns in the overall energy balance are the shell temperature (T_{sh}), the motor temperature (T_{mot}), the discharge temperature (T_d), and the mass flow rate (\dot{m}).

Refrigerant Gas

Figure 4 illustrates the heat transfer modes to the refrigerant gas inside the compressor shell. An energy balance on the gas yields the following equation:

$$\dot{Q}_{sh,c} + \dot{Q}_{m,c} + \dot{m} (i_{mi} - i_s) = \dot{Q}_{dl,c} + \dot{Q}_{mot,c} \quad (5)$$

where $\dot{Q}_{sh,c}$ is the convective heat transfer rate to the shell from the shell gas, $\dot{Q}_{m,c}$ is the convective heat transfer rate from the shell gas to the suction muffler, $\dot{Q}_{dl,c}$ is the convective heat transfer rate from the discharge line to the shell gas, $\dot{Q}_{mot,c}$ is the convective heat transfer rate from the motor and surrounding parts to the shell gas, and i_{mi} is the enthalpy of the suction gas entering the muffler.

The effective heat transfer coefficients between the suction gas and internal components inside the compressor h_{in} is determined from experimental data, so that

$$\dot{Q}_{sh,c} = h_{in} A_{sh} (T_{gas} - T_{sh}) \quad (6)$$

$$\dot{Q}_{mot,c} = h_{in} A_{mot} (T_{mot} - T_{gas}) \quad (7)$$

The heat transfer rates $\dot{Q}_{m,c}$ and $\dot{Q}_{dl,c}$ are part of the muffler and discharge line analysis. The muffler inlet temperature is related to a gas mixing parameter, δ , which is defined as the fraction of inlet gas that enters the muffler without mixing. A value of $\delta = 1$ represents a direct connect (no mixing) between the inlet and the muffler, while a value of $\delta = 0$ represents complete mixing. Thus,

$$\dot{m}_{tot} = \dot{m}_{sp} + \dot{m}_{dir} \quad (8)$$

$$\delta = \frac{\dot{m}_{dir}}{\dot{m}_{tot}} = 1 - \frac{\dot{m}_{sp}}{\dot{m}_{tot}} \quad (9)$$

If it is assumed that the spilled portion of the gas, m_{sp} , is heated to the shell gas temperature before it enters the muffler, that the specific heat of the gas does not vary over the temperature range, and that the temperature measurement at the muffler inlet is representative of a mixture of the direct and spilled gas, then from an energy and mass flow balance on the gas entering the muffler one obtains,

$$\delta = \frac{T_{gas} - T_{mi}}{T_{gas} - T_s} \quad (10)$$

where T_{mi} is the temperature of the gas mixture entering the muffler, and T_s is the temperature of the suction gas entering the compressor shell.

Suction Muffler

Heat transfer to the suction muffler is illustrated in Fig. 5 and includes convection from the shell gas and radiation from the motor. The energy balance for the muffler gives:

$$\dot{Q}_{m,c} + \dot{Q}_{m,r} = \dot{m}(i_{mo} - i_{mi}) \quad (11)$$

where $\dot{Q}_{m,c}$ is the convective heat transfer to the muffler from the shell gas, $\dot{Q}_{m,r}$ is the radiative heat transfer rate to the muffler from the motor, and i_{mo} is the suction gas enthalpy at the muffler outlet. Expressions for $\dot{Q}_{m,c}$ and $\dot{Q}_{m,r}$ are determined using the arithmetic mean temperature of the gas inside the muffler and the heat transfer resistance network illustrated in Fig. 5.

It is assumed that the only significant contribution to the radiation heat transfer comes from the motor surface which is immediately behind the muffler. The details of the muffler resistance network analysis are contained in Refs. 1 and 2. The muffler was analyzed in more detail than the other components inside the compressor to evaluate the effect of insulation on the gas temperature increase within the muffler.

Discharge Line

The heat transfer from the discharge line was determined from a series of finite elements as illustrated in Fig. 6. For each element the heat transfer rate is

$$\Delta \dot{Q}_{de} = \dot{m}(i_{in} - i_{out}) \quad (12)$$

The rate $\Delta \dot{Q}_{dl}$ includes both convection and radiation.

Motor, etc.

The control volume around the motor, oil and bottom of the shell, all of which are assumed to be at the same temperature, is shown in Fig. 7. The work input must balance the convective and radiative heat transfer and the enthalpy increase in the compression process. Thus,

$$\dot{W}_{in} = \dot{m}(i_{dp} - i_{mo}) + h_{in} A (T_{mot} - T_{gas}) + \dot{Q}_{bottom} + \epsilon A \sigma (T_{mot}^4 - T_{sh}^4) \quad (13)$$

Shell Top and Sides

The heat transfer modes to the top and sides of the shell are illustrated in Fig. 8. They include conduction from the refrigerant gas, radiation from the motor and discharge line, and heat transfer to the ambient.

COMPUTER CODE AND RESULTS

A computer program was written to solve for the temperatures of the motor surface (T_{mot}), shell (T_{sh}), and the gas temperature circulating inside the shell (T_{gas}), at the muffler inlet (T_{mi}), at the muffler outlet (T_{mo}), at the plenum discharge (T_{dp}) and at the discharge line leaving the shell (T_d). A constant volumetric efficiency, $\eta_v = 0.533$, was used to determine the mass flow rate, \dot{m} .

$$\dot{m} = \eta_v V \omega \rho_{mo} \quad (14)$$

where V is the swept volume of the compressor, ω is the rotational speed of the compressor motor, and ρ_{mo} is the density of the refrigerant at the muffler outlet.

The detailed analysis of the heat transfer in the suction and discharge plenum and in the compression piston was not included. Reference 8 is an analysis that could be integrated with this analysis to include those details. In the absence of that analysis a compression efficiency, η_{comp} , was used. The average value of $\eta_{comp} = 0.44$ obtained from the experimental program was used.

$$\eta_{comp} = \dot{m} (i_{dp} - i_{mo}) / \dot{w}_{in} \quad (15)$$

The experimentally determined value of the internal heat transfer coefficient that was used was

$$h_{in} = 8.6 \text{ Btu}/(\text{hr ft}^2 \text{ F}) \quad (16)$$

The computer program required an iterative solution. The iteration is on the mass flow rate. The gas circulation parameter, δ , and the suction line temperature, T_s , were varied parametrically to determine their effect on the temperatures and system performance.

The comparison of the computer program output with the experimental results of Ref. 3 are shown in Figs 9, 10, 11, and 12. Figure 9 shows the muffler outlet temperature vs the suction line temperature for various values of δ from 0.0 to 0.8. The calculated values of the muffler outlet temperature are consistently low but the trends (slope) match.

Figure 10 compares calculated and measured temperatures of the shell, motor, shell gas, muffler inlet, and muffler outlet as a function of δ . The experimental data actually has some scatter, partly due to different values of ambient temperatures. The values shown are for ambient temperatures near 72 F. The comparisons and trends are reasonably good except for the gas temperature at higher values of δ . The difference here is, we believe, due to the lack of a good heat transfer analysis for the plenum chambers and compression cylinder. It appears that the unsteady nature of the flow there produces effective heat transfer rates that are much higher than the steady-state values.

Figure 11 is a comparison of the mass flow rate for various values of δ . The theoretical (calculated) value shows a significant increase with increasing δ , whereas the experimental values show only a slight increase. The specific power consumption, shown in Fig. 12, can be directly related to the compressor efficiency. The expected decrease in specific power consumption with increasing δ is not

observed experimentally. Both the experimental and analytical results do indicate that decreasing δ (increasing the mixing inside the compressor shell) leads to decreased performance.

SUMMARY AND RECOMMENDATIONS

A modular computer program that accounts for the major modes of heat transfer between the compressor gas, the surroundings, and the major components of a small refrigeration compressor at steady-state operation has been developed. The computed temperatures of the compressor components and of the refrigerant gas at various points along the flow path are compared to experimental measurements over a range of operating conditions. The computer program predicts temperatures and trends with reasonable accuracy, but some obvious discrepancies are present.

The major deficiencies of the present model appear to be that the heat transfer in the suction plenum, compression cylinder, and discharge plenum is not modeled adequately. To adequately model the heat transfer in this region requires an unsteady analysis that adequately accounts for the increased heat transfer to or from a pulsating flow. There are other aspects of the operation that are not included in the analysis such as heat transfer due to vaporization and condensation of the lubricating oil and flow leakage around the compression cylinder.

The modular nature of the computer program makes it feasible to incorporate improvements modularly, while retaining the overall framework of the analysis. Different refrigerant gases can be investigated by replacing the thermodynamic data subroutine. However, that change does not account for the differences in heat transfer coefficients which would result from the use of a different refrigerant gas. The effective heat transfer coefficients were determined experimentally.

It is the opinion of the authors that the computer program described herein can be used to obtain comparative results, and can serve as a framework around which a more detailed analysis can be developed for design studies.

ACKNOWLEDGMENT

This research project was sponsored by NECCHI, S.p.A.

REFERENCES

1. Meyer, W.A., "An investigation into Heat Transfer Processes in a Small Hermetic Refrigeration Compressor," MSME, Purdue University, 1987.
2. Meyer, W.A., and Thompson, H. D., "An Investigation into Heat Transfer Processes in a Small Hermetic Refrigeration Compressor," Ray W. Herrick Laboratories Report No. 0891-3, HL87-16P, May 1987
3. Meyer, W.A., and Thompson, H. Doyle, "An Experimental Investigation Into Heat Transfer to the Suction Gas in a Low-Side Hermetic Refrigeration Compressor, "Paper presented at the 1988 International Compressor Conference, Purdue University, W. Lafayette, IN, July 18-21, 1988.
4. Srikanth, Ramanujam, "How the Design of the Suction Return Affects Compressor Efficiency," MSME, Purdue University, 1987.
5. Srikanth, R. and Thompson, H.D., "How the Design of the Suction Return Affects Compressor Efficiency," Ray W. Herrick Laboratories Report 0891-4, HL87-17P, May 1987.

6. Srikanth, Ramanujam, and Thompson, H. Doyle, "How the Design of the Suction Return Affects Compressor Efficiency," Paper presented at the 1988 International Compressor Engineering Conference, Purdue University, W. Lafayette, IN, July 18-21, 1988.

7. Incropera, Frank P. and David P. Dewitt, Fundamentals of Heat and Mass Transfer, 2nd ed., New York: John Wiley and Sons, 1985.

8. Morel, T., and Keribar, R., "Heat Transfer and Component Temperature Prediction in Reciprocating Compressors," Paper presented at the 1988 International Compressor Engineering Conference, Purdue University, W. Lafayette, IN, July 18-21, 1988.

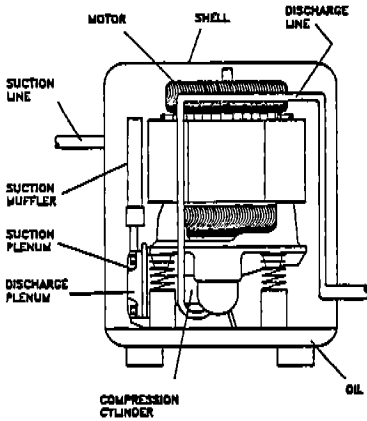


Figure 1: Schematic of a Normal Compressor Showing Major Internal Parts

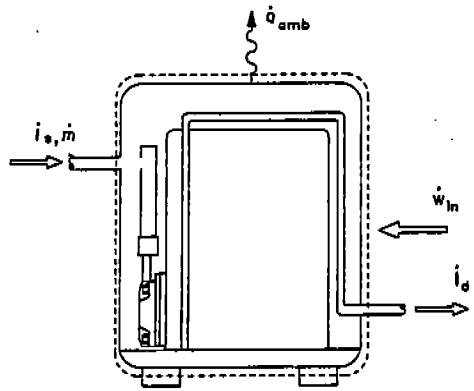


Figure 2: Schematic of Compressor Illustrating the Overall Energy Balance

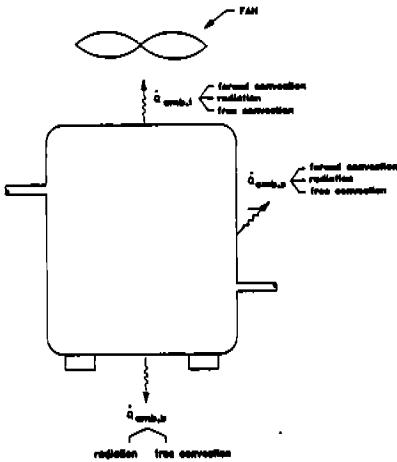


Figure 3: Schematic of Compressor Showing the Modes of Heat Transfer to the Ambient

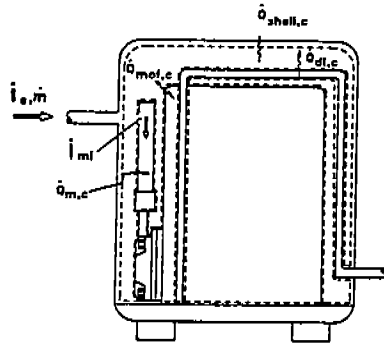


Figure 4: Schematic of Compressor Illustrating the Shell Gas Energy Balance

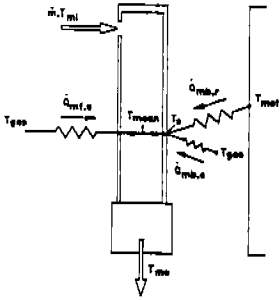


Figure 5: Resistance Network Used to Analyze the Heat Transfer to the Suction Muffler

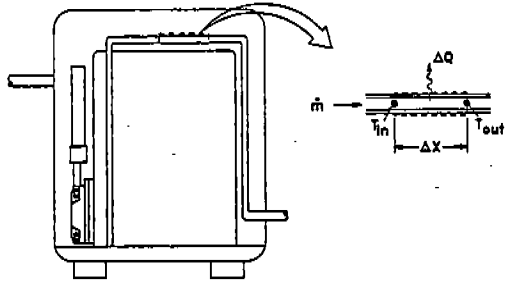


Figure 6: Schematic of Compressor Illustrating the Energy Balance on a Finite Section of Discharge Line

Figure 7: Schematic of Compressor Illustrating the Energy Balance on the Motor/Oil

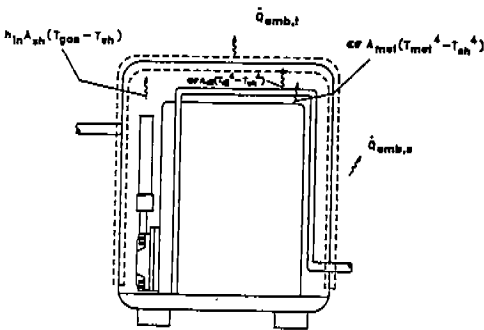
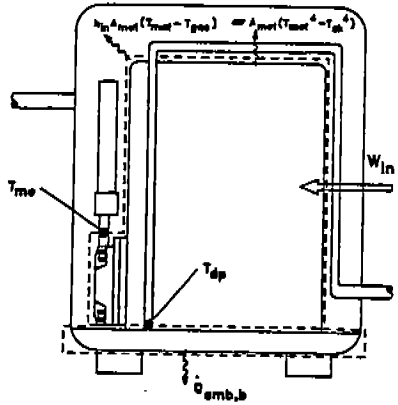


Figure 8: Schematic of Compressor Illustrating the Energy Balance on the Compressor Shell

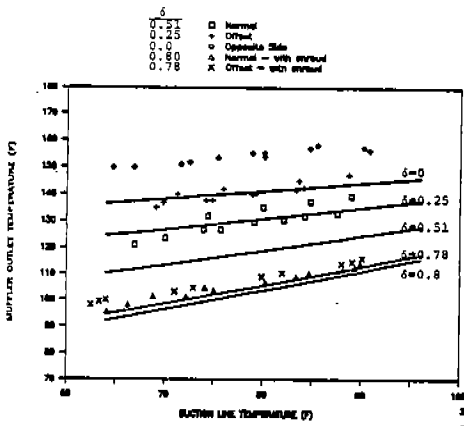


Figure 9: Muffler Outlet Temp. as a Function of Suction Line Temp. (Analytical & Experimental Results)

Figure 10: Component and Gas Temps as a Function of δ (Analytical & Experimental Results)

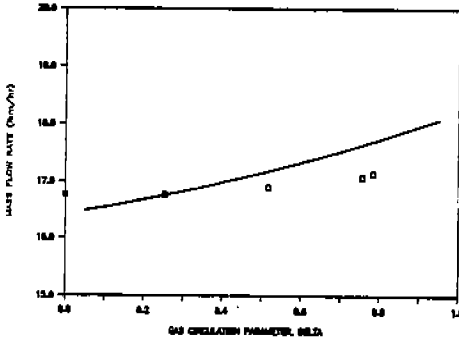
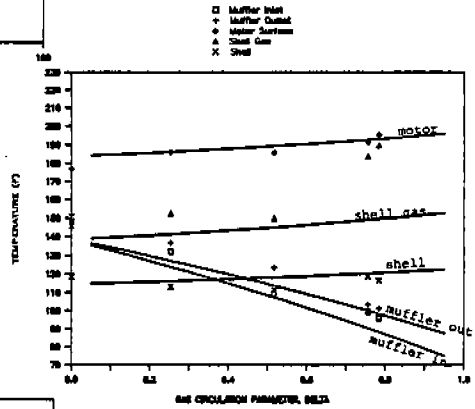


Figure 11: Mass Flow Rate as a Function of δ (Analytical & Experimental Results)

Figure 12: Specific Power Consumption as a Function of δ (Analytical & Experimental Results)

